Generation of correlated photon pairs in type-II parametric down conversion – revisited

Christian Kurtsiefer[1], Markus Oberparleiter[1], and Harald Weinfurter[1,2]

February 7, 2001

submitted to J. Mod. Opt.

Abstract

Type-II parametric down conversion in nonlinear optical crystals has turned out to be one of the most powerful methods to generate entangled photon pairs, and even allowed a large set of experiments on foundations of quantum mechanics and recent applications in quantum communication. In this paper, we present an experimental investigation of the emission characteristics for down-converted photons in order to investigate the possibility of high brightness sources for correlated photon pairs. Furthermore, we discuss possible ways to increase the collection efficiency for polarisation entangled photon pairs.

1 Introduction

One of the most successful techniques to generate entangled, distinguishable particles is the generation of polarisation-entangled photons in type-II parametric down conversion[1]. With such sources, a whole range of recent experiments demonstrating fundamental concepts in quantum mechanics based on entanglement, like testing Bell inequalities[2, 3] over a long distance and quantum dense coding[4] was carried out. The process was also used to generate entangled states of more than two distinguishable particles, and to experimentally demonstrate entanglement swapping[5], quantum teleportation[6] and the preparation of a GHZ[7] state of space-like separated particles. Furthermore, quantum cryptography has been considered[8] and demonstrated [9, 10] as an application for entangled photon pairs. All of these applications require a large number of photon pairs, but up to now, large pair generation rates have been achieved mainly with type-I parametric conversion sources[11, 12, 13], where both of the photons (signal and idler) are emitted with the same polarisation, and thus do not directly form a polarisation-entangled state.

Various attempts have been made to increase the available rate of correlated photons, like focusing the pump beam[14], using cylindrical optics[15] or resonant enhancement of the pump beam[16]. In this article, we report on an experimental investigation of type-II parametric fluorescence in BBO as a nonlinear optical crystal pumped in the UV, where the aim was to maximise the pair rates emitted in a wavelength interval around the degeneracy wavelength in the near-infrared region into the two optical channels used for detection.

2 Phase matching condition

The basic optical configuration used for type-II down conversion is shown in figure 1. A pump beam enters a nonlinear optical crystal as an e-polarised beam, and is partially

[1] Sektion Physik, Ludwig-Maximilians-Universität, D-80797 München, Germany
[2] Max-Planck-Insitut für Quantenoptik, D-85748 Garching, Germany

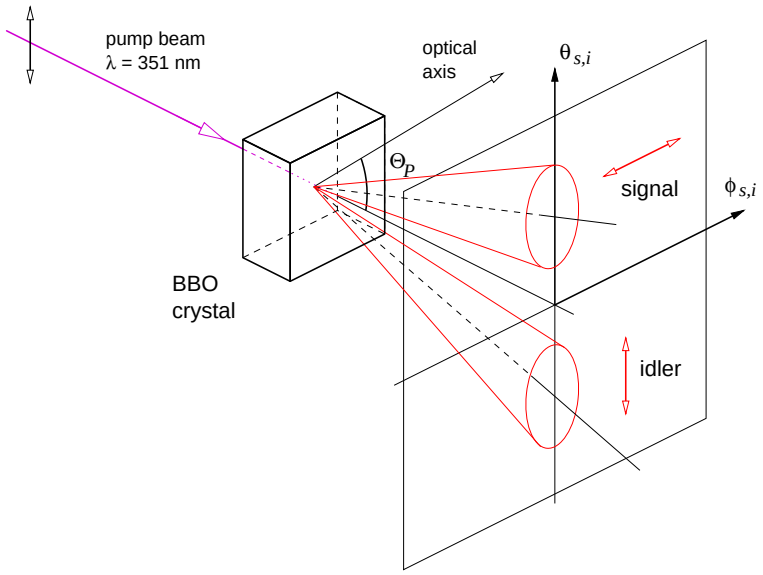

Figure 1: Geometrical arrangement for type-II parametric down conversion. A collimated UV pump beam is sent as e-polarisation in a nonlinear optical crystal. Due to parametric conversion, pair photons are generated, which are emitted in a manyfold of two cones for a given wavelength, referred to as signal and idler, where one of the cones is polarised in e direction, and the other one in o-direction.

converted into pairs of photons, obeying energy and momentum conservation. For a fixed pump wave vector, for a crystal with dimensions much larger than the optical wavelength, and for a fixed wavelength λ_S of the e-polarised photon (referred to as signal here), the emission direction of this photon and the one of the o-polarised photon (referred to as idler) are emitted into a one-dimensional manifold of corresponding directions, where both signal and idler photons form a cone of wave vectors. To obtain entangled photon pairs from a monochromatic pump with a wavelength λ_P, the pump direction is chosen such that the two cones corresponding to wavelengths $\lambda_s = \lambda_i = 2\lambda_P$ of signal and idler overlap for two directions[1].

In a practical experiment, one will allow for a certain bandwidth $\Delta\lambda$ around the degeneracy wavelength $2\lambda_P$ for both signal and idler light. This causes signal and idler light to be emitted in a wider set of directions, resulting in an angular width $\Delta\alpha$ of the emission cones (see figure 2(a)).

As a detailed analysis of the phase matching conditions has been given before[17, 18], we only give a rough sketch of the calculation necessary to obtain the angular distribution of signal- and idler photons as a function of the collected spectrum, restricted to uniaxial nonlinear crystals such as BBO.

To simplify the calculation, we restrict the wave vectors of pump, signal and idler waves into the plane containing both the pump wave vector and the optical axis of the nonlinear (uniaxial) crystal. The conditions for energy and momentum conservation,

$$\omega_P = \omega_s + \omega_i \,, \tag{1}$$

$$\mathbf{k}_P = \mathbf{k}_s + \mathbf{k}_i \tag{2}$$

can be combined to one single equation:

$$\left(\frac{n_{e,i}\, n_{o,i}\, \omega_i \cdot z_i}{\sqrt{n_{o,i}^2 + (n_{e,i}^2 - n_{o,i}^2)\, z_i^2}} - \tilde{n}_P\, \omega_P \cdot z_p \right)^2 +$$

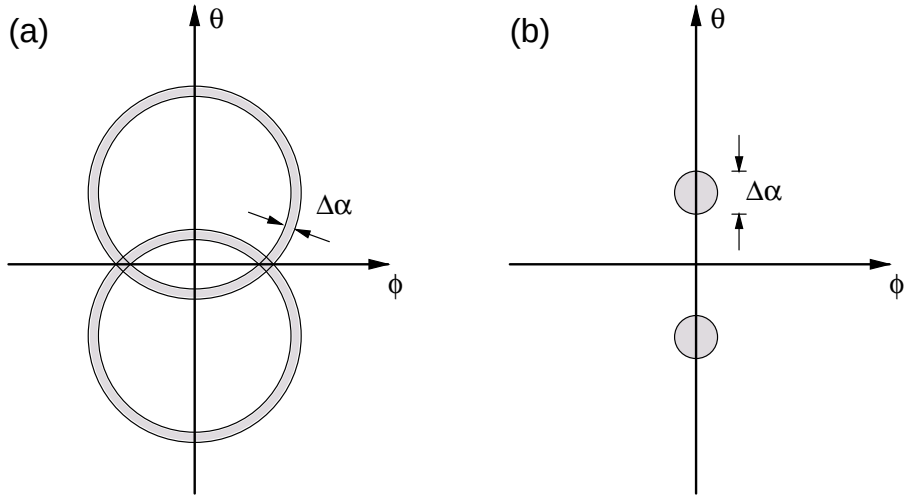

Figure 2: Angular width of parametric fluorescence for a given spectral bandwidth $\Delta\lambda$ of signal and idler light. (a) In the configuration used for entangled photon generation, phase matching allows for two rings with an angular width of $\Delta\alpha$. (b) For a larger angle between pump beam and optical axis, two circular regions with a diameter $\Delta\alpha$ are expected.

$$\left(\frac{n_{e,i}\, n_{o,i}\, \omega_i \cdot \sqrt{1-z_i^2}}{\sqrt{n_{o,i}^2 + (n_{e,i}^2 - n_{o,i}^2)\, z_i^2}} - \tilde{n}_P\, \omega_P \cdot \sqrt{1-z_p^2} \right)^2 = n_{o,s}^2\, (\omega_p - \omega_i)^2 \quad (3)$$

Therein, $n_{e,i}$ and $n_{o,i}$ denote the extraordinary and ordinary refractive index at the idler frequency ω_i, and $n_{o,s}$ the ordinary refractive index of the conversion crystal at the signal frequency $\omega_s = \omega_P - \omega_i$. The effective refractive index for the pump, $\tilde{n}_P$, is given by

$$\tilde{n}_P = \frac{n_{e,p}\, n_{o,p}}{\sqrt{n_{o,p}^2 + (n_{e,p}^2 - n_{o,p}^2)\, z_p^2}} \quad , \quad (4)$$

where $n_{e,p}$ and $n_{o,p}$ are extraordinary and ordinary refractive index at the pump wavelength. The directions of pump and idler beam are characterised by their directional cosines $z_p = \cos(\Theta_P)$ and $z_i = \cos(\Theta_i)$, where Θ_P and Θ_i are the angles inside the crystal between the optical axis and the propagation of pump and idler, respectively.

For a given pump orientation Θ_P, pump frequency ω_p and idler frequency ω_i, the refractive indices are given by Sellmeier equations[19], and equation (3) can be used to determine the directional cosine z_i of the idler. For a proper choice of the pump direction z_p, two real solutions for z_i can be found.

To calculate the emission direction outside a crystal cut with end faces normal to the pump direction, Snell's law has to be considered for non-normal emission. Doing so, we end up with two solutions for the external emission angle θ_i (and two corresponding solutions for the signal emission angle θ_s), measured with respect to the pump beam. For a pump wavelength of $\lambda_P = 351.1$ nm, numerical values for $\theta_i(\lambda_P, \Theta_P; \lambda_i)$ as a function of idler wavelength λ_i are shown in figure 3. Due to momentum conservation, the corresponding external signal emission angle is given by $\theta_s = -\theta_i$.

If signal and idler momentum are not restricted to the plane containing the pump direction and the optical axis, all values of θ_i between the two solutions of equation (3) can be taken, forming two rings in a plane perpendicular to the pump direction, as symbolised in figure 1.

For a pump angle of $\Theta_P = 48.1°$, the idler angle θ_i is restricted to negative values. Therefore, signal and idler light form two non-intersecting rings, while for an angle of

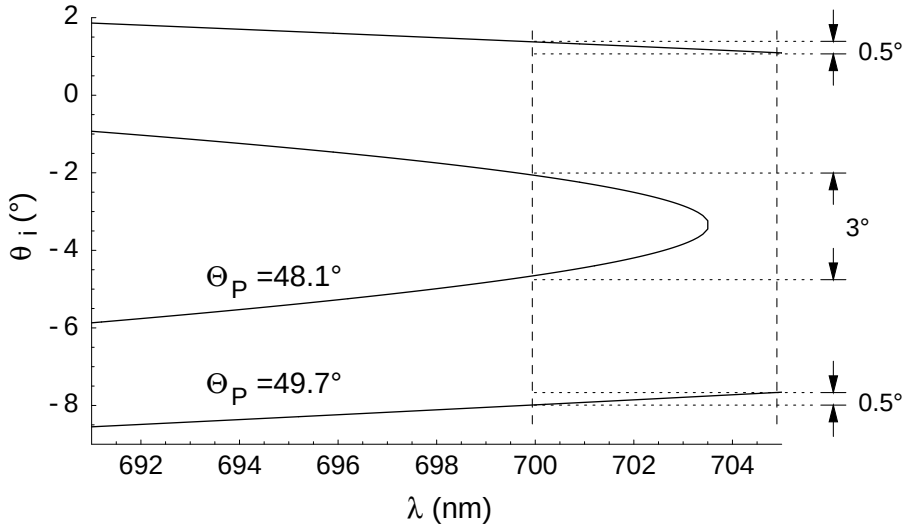

Figure 3: Calculated phase matching condition for the idler wave (in the plane containing the optical axis, i.e., $\phi_i = 0°$) for a pump wavelength of $\lambda_P = 351.1$ nm. For a pump beam orientation of $\Theta_P = 48.1°$, a wavelength interval of 5.5 nm around the degeneracy wavelength forms a continuous region, where for a larger pump angle Θ_p two distinct regions corresponding to a cut through the ring pattern are formed.

$\Theta_P = 49.7°$, the allowed interval for θ_i (and thus also for θ_s) contains $\theta_i = 0°$, the rings intersect, and allow for extraction of polarisation-entangled photon pairs.

To obtain the geometrical width $\Delta\alpha$ of the emission patterns for a given spectral range for signal and idler as sketched in figure 2, we use the dispersion relation $\theta_i(\lambda_P, \Theta_P; \lambda_i)$ as shown in figure 3. For an interference filter with a transmission spectrum centred around the degeneracy wavelength of 702.2 nm and a width of 5.5 nm (FWHM), a pump beam orientation of $\Theta_P = 48.1°$ leads to the down-converted light being emitted in two circular areas with diameter of $\approx 3°$, whereas for the other displayed pump orientation, $\Theta_P = 49.7°$, a ring with a diameter of $\approx 9°$ and a width of $\approx 0.5°$ is formed by both signal and idler light.

3 Measurement of the angular distribution

To experimentally investigate the momentum distribution of the down-converted light for different crystal orientations, we observe only single count rates rather than coincidence events necessary to identify entangled photon pairs. However, this is sufficient to understand the spectral and spatial behaviour of the parametric down conversion process for the purpose of maximising the rate of available photon pairs in an experiment.

Our experimental set-up is shown in figure 4. A collimated UV pump beam from an Ar ion laser ($\lambda = 351.1$ nm) with a beam waist of $w_p = 510\ \mu$m and a pump power of 100 mW is entering a BBO crystal of thickness $d = 2$ mm. As the dimensions of the interaction volume between pump and down-converted waves exceed the optical wavelengths in the crystal by far, momentum uncertainty due to the finite crystal size should be negligible. The angular distribution of the Gaussian pump beam corresponds to $\Theta_D = 0.03°$ FWHM, and thus the pump can be treated as a plane wave with good approximation[20]. The crystal is cut to have an angle of $\Theta_P^{(0)} = 49.2°$ with the surface normal, closely corresponding to the angle for degenerate collinear down conversion. A subsequent dielectric mirror M is reflecting out the residual pump beam, and transmitting light from parametric down

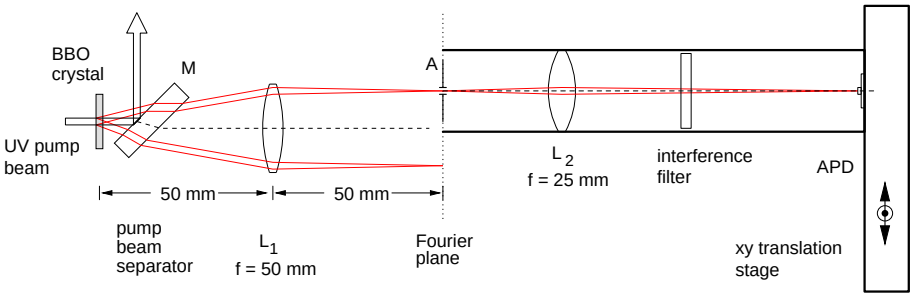

Figure 4: Experimental setup to investigate the angular intensity distribution $I(\theta, \phi)$ of down-converted photons. After a pump beam separator M (a dielectric mirror reflecting off UV light) the angular distribution of the down-converted light is transformed into a spatial distribution with a lens L_1 of focal length $f = 50$ mm. The intensity distribution for a spectral range defined by an interference filter in that plane is probed with a passively quenched Avalanche photodiode (APD). A relay lens L_2 is used to match the desired spatial resolution in the Fourier plane to the sensitive area of the APD.

conversion. A Fourier transform lens L_1 with a focal length of $f = 50$ mm converts the angular distribution of the down-converted light being emitted in a range of $20° \times 20°$ to a spatial distribution of roughly 17×17 mm^2, which is probed with a Silicon Avalanche Photodiode (APD). In order to obtain a sufficient angular resolution, we used an imaging lens L_2 with a focal length of $f = 25$ mm to enlarge a probe area in the Fourier plane from 200 μm to the active diameter of 500 μm of the APD. The relay lens, the Avalanche diode, and an auxiliary aperture of diameter < 1 mm to minimise stray light impinging on the APD were mounted on a 2D linear translation stage with motorised micrometer screws. To define the spectral bandwidth of the down-converted light collected with this setup, we inserted an interference filter with a bandwidth of 5.5 nm FWHM around the degeneracy wavelength of 702.2 nm into the optical path. The filter was located outside the Fourier plane to minimise the effect of fluorescence from residual UV light.

With this setup, we determined the intensity distribution $I(\theta, \phi)$ for different orientations of the conversion crystal relative to the pump beam. We denote the orientations by their deviation $\Delta\Theta = \Theta_P - \Theta_P^{(0)}$ of the pump direction inside the crystal from the normal of the end faces; the value was obtained by correcting the external tilt angle of the BBO crystal by the refractive index for the pump. The corresponding intensity distributions are shown in figure 5. For $\Delta\Theta < 0°$, the two emission cones of signal and idler manifold are separated. At an angle of $\Delta\Theta = -0.88°$, the rings collapse into two circular blobs. The width of these emission areas can be extracted from a vertical cut ($\phi = 0°$) as shown in the left part of figure 6 to be $\approx 3°$. This is in good agreement with what is expected from the phase matching curve obtained for a pump beam orientation of $\Theta_P = 48.1°$ in figure 3. For $\Delta\Theta = 0°$, the two rings of signal and idler touch at $\theta = 0°$, whereas for $\Delta\Theta > 0°$, two intersecting rings are observed. With increasing angle $\Delta\Theta$, the diameter of the signal and idler rings increase further, while their widths decrease. For $\Delta\Theta = +0.44°$, the observed width of $\approx 0.5°$ of a ring (see right part of figure 6) corresponds to the calculated width of the second trace in figure 3, reflecting the shallower slope of $\theta_i(\lambda_i)$ at larger opening angles.

The peak intensity of the measured angular distribution of down-converted light changed only slightly with the different pump angles; this is in agreement with expressions for a linear dependence of the fluorescence intensities from the effective nonlinear susceptibility χ_{ijk}^{eff} [21, 22]. Assuming pump, signal and idler beams being collinear, χ_{ijk}^{eff} is expected to vary with $\cos^2 \Theta_P$[23], which would correspond to a variation of only 6.5% over the investigated range of pump angles Θ_P. However, we observe for all angles Θ_P an inten-

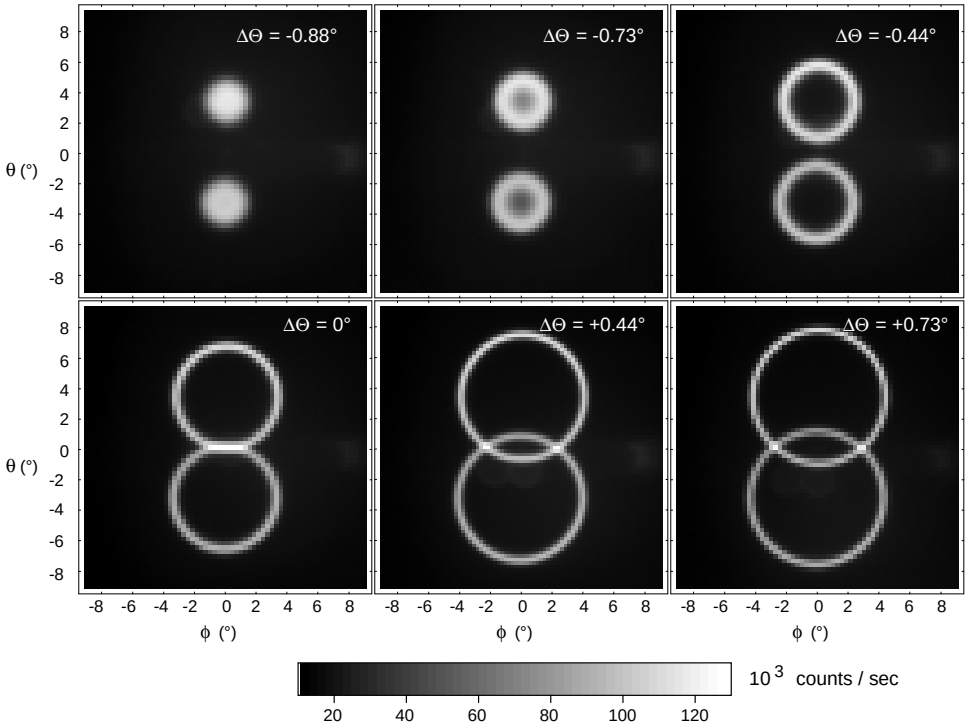

Figure 5: Measured intensity distribution of down-converted light for different conversion crystal orientations; $\Delta\Theta = 0°$ corresponds to normal incidence on the crystal faces, corresponding to a configuration where signal and idler component approximately co-propagate with the pump beam (corresponding to an angle $\phi = \theta = 0°$). In the first row, the cones for signal and idler light never intersect, while for the last two distributions, there are two intersection directions for $\theta = 0°$, allowing to collect polarisation-entangled photon pairs.

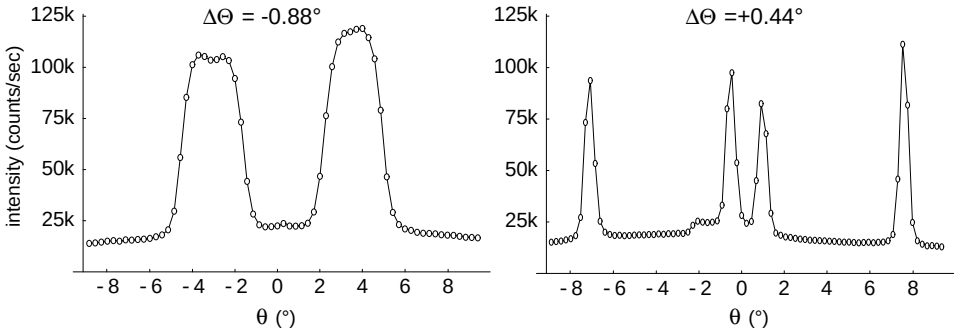

Figure 6: Intensity distribution for two particular crystal orientations. For the two-blob-case corresponding to $\Delta\Theta = -0.88°$, the angular intensity is only slightly larger than for the intersecting-ring case, corresponding to $\Delta\Theta = +0.44°$.

sity difference for the signal and idler ring of about 20%, probably due to the different transmission of the pump beam separator M for s- and p-polarised light.

4 Collection efficiencies

In order to discuss the strategy for optimising photon collection, it is useful to first interpret our measurements in terms of the brightness B of the the parametric down conversion source. That quantity describes the number of fluorescence photons emitted per time, source area and solid angle, and may be regarded as a measure for an optical phase space density. Here, we use the formalism only in a qualitative way; tools for a more rigorous treatment can be found in [24]. We restrict ourselves to only one partner of the photon pair, e.g., the idler, so there should be no spatial coherence in the source other than the limits for the momentum distribution defined by the phase matching condition and the spectral bandwidth of the collected light. Furthermore, we simplify the spatial origin of the fluorescence light as a plane defined by the pump beam crossing a thin crystal. We then assume that the phase space density or brightness $B(\theta, \phi; x, y)$ of the emitted light separates in source coordinates x, y and emission angles θ, ϕ, and obtain:

$$B(\theta, \phi; x, y) = \frac{I(\theta, \phi)}{\Omega_c} \cdot \frac{\pi w_p^2}{2} e^{-2r^2/w_p^2} \tag{5}$$

In this expression, $I(\theta, \phi)$ is the observed or calculated angular distribution of light, Ω_c is the acceptance solid angle of our detector (fixed by the de-magnified detector diameter and the focal length of the Fourier lens L_1 to a numerical value of $\Omega_c = 1.26 \cdot 10^{-5}$ sr), w_p denotes the waist of the Gaussian pump beam, and $r = \sqrt{x^2 + y^2}$ is the radial position in the source plane. Expression (5) implies that the observed photon count rate $I(\theta, \phi)$ is a direct measure for the brightness $B(\theta, \phi; x, y)$. As pointed out, this varies only slightly with the pump orientation $\Delta\Theta$. An apparently higher intensity of the rings with smaller diameters, as observed in photographic exposures of type-II parametric conversion[25], is not equivalent to a higher brightness.

Let us now consider a case where photon pairs are to be collected into single spatial modes, as e.g. defined by single mode optical fibres, or in images thereof. The acceptance area in phase space for such modes (assumed to be Gaussian) is limited to Gaussian distributions with a fixed product of spatial extent and divergence angle, manifested in the relation

$$\theta_D = \frac{\lambda}{\pi w_0} \tag{6}$$

between the divergence θ_D and the minimum waist w_o of a beam. In order to optimise the number of photons collected per time, the source brightness has to be tailored to have a maximal overlap with an acceptance function $\zeta(\theta, \phi; x, y)$ of the Gaussian mode. As the angular distribution to the brightness $B(\theta, \phi; x, y)$ is fixed by the phase matching condition for a given spectral bandwidth of the light to be collected, the only free parameter to achieve this adjustment is the source are defined by the pump waist. We shall illustrate this for the important example of collecting entangled photon pairs in the figure-of-eight configuration as in[1]:

First, the orientation of the pump beam is fixed such that the two rings of signal and idler intersect perpendicularly (i.e., $\partial\phi_s/\partial\theta_s = -\partial\phi_i/\partial\theta_s = \pm 1$ for the intersection directions). For a BBO crystal pumped with $\lambda = 351.1$ nm, this corresponds to a pump angle of $\theta_P = 49.7°$. Then, the angular width corresponding to the desired spectral width $\Delta\lambda$ is calculated by linearising the phase matching ratio around the degeneracy wavelength $2\lambda_P$. For the given example, we obtain $|d\theta_i/d\lambda_i| = 0.55$ °/nm. For a Gaussian spectral distribution, this results in a Gaussian distribution of emission angles around the ring defined by the degeneracy wavelength. This is also the case for the other photon, and as the rings

intersect perpendicularly, the angular region to be collected is a Gaussian distribution with rotational symmetry around the intersection direction of the degenerate wavelength, with a divergence given by θ_i. This divergence fixes the divergence θ_D of the Gaussian target mode and therefore its waist w_0. To obtain the maximal brightness from the (incoherently) fluorescing source associated with the parametric conversion process, the pump light can be restricted to a source area corresponding to the minimal cross section of the Gaussian mode. With this technique, coincidence count rates of 360000 s^{-1} polarisation-entangled photon pairs have been observed at a pump power of $P = 460$ mW impinging on a 2 mm thick BBO crystal[26].

Another interesting optimisation problem is posed by the attempt of collecting all the light produced by parametric down conversion. Such a configuration would be a convenient source of correlated photon pairs, where each of the photons is emitted in a distinct polarisation, in contrast to efficient photon pair sources using type-I parametric down conversion[11, 12, 13]. It seems natural to consider the two-blob configuration for that purpose, as observed experimentally for $\Delta\Theta = -0.88°$ in figure 5, because there the angular distribution of the light is close to a Gaussian distribution, and one could hope for a large coupling efficiency into a single Gaussian mode. However, the highly dispersive phase matching condition leads to a large angular spread for a bandwidth of 5 nm. This implies that only photons originating from a very narrow source area can be collected into that mode. This implies that the pump has to be focused to a very small beam waist, eventually causing problems with the damage threshold of the nonlinear crystal. Also, the phase matching condition is getting more complicated, since a tightly focused pump beam cannot be treated as a plane wave any more[14, 20].

The situation is different if the light can be collected into multi-mode fibres. For example, for a standard multi-mode fibre with a numerical aperture of $NA = 0.22$ and a core diameter of $D = 50$ μm, the source brightness $B(\theta, \phi; x, y)$ could extend over a mode acceptance function $\zeta(\theta, \phi; x, y)$ in phase space, which is given by:

$$\zeta(\theta,\phi;x,y) = \left\{ \begin{array}{ll} 1, & x^2+y^2 < D^2/4 \\ 0, & \text{otherwhise} \end{array} \right\} \cdot \left\{ \begin{array}{ll} 1, & \theta^2+\phi^2 < \arctan^2(NA/2) \\ 0, & \text{otherwhise} \end{array} \right\}$$

This corresponds to a phase space volume $\mathcal{V}$ of

$$\mathcal{V} = \int d\theta d\phi \int\limits_{\text{source}} dx dy \zeta(\theta,\phi;x,y) \approx 74\,\mu\text{m}^2 \quad ,$$

or a "transverse mode capacity" of $\mathcal{V}/(\lambda^2/4) \approx 600$ (single) modes at a wavelength of 702.2 nm. In order to maximise the overlap between source brightness and acceptance function, the constraints to the source area are much more relaxed, so this method may successfully be implemented to obtain a strong source for correlated (but not polarisation-entangled) photons.

5 Summary

We presented an experimental investigation of the fluorescence brightness in type-II parametric conversion for different orientations of the pump beam relative to the optical axis of a BBO nonlinear optical crystal. We found good agreement between our experiments and the angular distributions calculated from the phase matching conditions. We conclude that collection of correlated photon pairs can be optimised by observing the source brightness function $B(\theta, \phi; x, y)$, and adjusting the free parameters therein to the acceptance region of a target mode in phase space. For collecting polarisation-entangled photon pairs, this has been demonstrated successfully[26]. Optimising collection of all the light form type-II parametric down conversion for crystal orientations leading to well-separated emission

directions of signal and idler light can result in high efficiencies when coupling into multi-mode fibres, but may be difficult if the light should be collected into single spatial modes. Whereas just for the creation of photon pairs other recently developed techniques could be favourable[12, 13], up to now non-collinear type-II phase matching seems still to be the best source for polarisation-entangled photons.

Acknowledgements

This work was supported by the European Union in the FET/QuComm research project (IST-1999-10033) and the Deutsche Forschungsgemeinschaft.

References

[1] P.G. Kwiat, K. Mattle, H. Weinfurter, A. Zeilinger, A.V. Sergienko, Y. Shih, 1995, *Phys. Rev. Lett.,* **75**, 4337.

[2] P.R. Tapster, J.G. Rarity, and P.C.M. Owens, 1994, *Phys. Rev. Lett.,* **73**, 1923.

[3] G. Weihs, T. Jennewein, C. Simon, H. Weinfurter, and A. Zeilinger, 1998, *Phys. Rev. Lett.,* **81**, 5039.

[4] K. Mattle, H. Weinfurter, P.G. Kwiat, A. Zeilinger, 1996, *Phys. Rev. Lett.,* **76**, 4656.

[5] J.-W. Pan, D. Bouwmeester, H. Weinfurter, and A. Zeilinger, 1998, *Phys. Rev. Lett.,* **80**, 3891.

[6] D. Bouwmeester, J.-W. Pan, K. Mattle, M. Eibl, H. Weinfurter, and A. Zeilinger, 1997, *Nature,* **390**, 576.

[7] D. Bouwmeester, J.-W. Pan, M. Daniell, H. Weinfurter, and A. Zeilinger, 1999, *Phys. Rev. Lett.,* **82**, 1345.

[8] A.K. Ekert, 1991, *Phys. Rev. Lett.,* **67**, 661.

[9] A.K. Ekert, J.G. Rarity, P.R. Tapster, and G.M. Palma, 1992, *Phys. Rev. Lett.,* **69**, 1293.

[10] T. Jennewein, Ch. Simon, G. Weihs, H. Weinfurter, and A. Zeilinger, 2000, *Phys. Rev. Lett.,* **84**, 4729.

[11] P.G. Kwiat, E. Waks, A.G. White, I. Appelbaum, P.H. Eberhard, 1999, *Phys. Rev. A,* **60**, R773.

[12] S. Tanzilli, H. de Riedmatten, W. Tittel, H. Zbinden, P. Baldi, M. de Micheli, D.B. Ostrowski and N. Gisin, 2001, *Electronics Letters*, **37**, 26-28.

[13] K. Sanaka, K. Kawahara, and T. Kuga, 2000, preprint at http://arXiv.org/abs/quant-ph/0012028.

[14] C.H. Monken, P.H. Suoto Ribeiro, and S. Pádua, 1998, *Phys. Rev. A,* **57**, R2267.

[15] P.G. Kwiat, private communication.

[16] M. Oberparleiter, H. Weinfurter, 2000, *Opt. Com.,* **183**, 133.

[17] P.G. Kwiat, P.H. Eberhard, A.M. Steinberg, and R.Y. Chiao, 1994, *Phys. Rev. A,* **49**, 3209.

[18] M.H. Rubin, 1996, *Phys. Rev. A*, **54**, 5349.

[19] D. Eimerl, L. Davis, S. Velsko, E.K. Graham, and A. Zalkin, 1987, *J. Appl. Phys.*, **62**, 1968.

[20] T.B. Pittman, D.V. Strekalov, D.N. Klyshko, M.H. Rubin A.V. Sergienko, and Y.H. Shih, 1996, *Phys. Rev. A*, **53**, 2804.

[21] A. Yariv, 1989, *Quantum Electronics*, Third edition, (New York: J. Wiley& Sons).

[22] C.K. Young and L. Mandel, 1985, *Phys. Rev. A*, **31**, 2409.

[23] V.G. Dimitriev, G.G. Gurzadyan, and D.N. Nikogosyan, 1999, *Handbook of Nonlinear Optical Crystals*, Third edition, (Berlin: Springer Verlag).

[24] l. Mandel and E. Wolf, 1995, *Optical coherence and quantum optics*, (Cambridge: Cambdidge University Press).

[25] See for example the cover picture of D. Bouwmeester, A. Ekert, and A. Zeilinger, 2000, *The physics of Quantum Information*, (Berlin: Springer Verlag).

[26] Ch. Kurtsiefer, M. Oberparleiter, and H. Weinfurter, 2001, *submitted to Phys. Rev. A*, preprint at http://arXiv.org/abs/quant-ph/0101074.